Characterization of the $S=9$ excited state in Fe_8Br_8 by electron paramagnetic resonance

D. Zipse, J. M. North, and N. S. Dalal
Department of Chemistry and Biochemistry and National High Magnetic Field Laboratory, Florida State University, Tallahassee, Florida 32306, USA

S. Hill and R. S. Edwards
Department of Physics, University of Florida, Gainesville, Florida 32611-8440, USA
(Received 1 August 2003; published 7 November 2003)

High-frequency electron paramagnetic resonance has been used to observe the magnetic dipole, $\Delta M_s = \pm 1$, transitions in the $S=9$ excited state of the single-molecule magnet Fe_8Br_8. A Boltzmann analysis of the measured intensities locates it at 24 ± 2 K above the $S=10$ ground state, while the line positions yield its magnetic parameters $D=-0.27$ K, $E=\pm 0.05$ K, and $B_4^0=-1.3\times10^{-6}$ K. D is thus smaller by 8% and E larger by 7% than for $S=10$. The anisotropy barrier for $S=9$ is estimated as 22 K, which is 25% smaller than that for $S=10$ (29 K). These data also help assign the spin exchange constants (J's) and thus provide a basis for improved electronic structure calculations on Fe_8Br_8.

DOI: 10.1103/PhysRevB.68.184408 PACS number(s): 75.50.Xx, 75.60.Jk, 75.75.+a, 76.30.−v

I. INTRODUCTION

Single-molecule magnets (SMM's), defined as compounds where a magnetic domain can, in principle, be reduced to a single molecule,[1,2] have recently been of high theoretical and experimental interest due to their novel properties and potential applications, which include quantum tunneling of their magnetization (QTM),[3–6] whose detailed mechanism is still not fully understood, molecular memory devices,[7,8] and elements of quantum computers.[9] One of the best characterized SMM's is $[(C_6H_{15}N_3)_6Fe_8(\mu_3\text{-}O)_2(\mu_2\text{-}OH)_{12}]Br_7(H_2O)Br\cdot 8H_2O$, abbreviated Fe_8Br_8,[10,11] whose main spin-bearing skeleton is shown in Fig. 1.

Studies by magnetization,[12] neutron scattering,[13,14] electron paramagnetic resonance (EPR),[11,15–21] and NMR (Ref. 22) techniques have established that the ground state has a spin value $S=10$. Figure 1 shows a schematic of the spin configuration of the Fe^{3+} ($S=5/2$) ions. At temperatures below 1 K, the magnetization relaxation takes places via QTM.[4] While a great deal of progress has been made in understanding the nature of QTM in Fe_8Br_8, many questions still remain unclear. For example, the magnitudes of calculated tunneling rates are much lower than the observed values.[23] Second, there is a lack of data on the nature and magnitude of the spin-exchange constants J's between the eight Fe^{3+} ions in the Fe_8Br_8 core. The best estimates come from the temperature dependence of the dc magnetic susceptibility χ_{dc}.[12,24] The χ_{dc} (Ref. 12) could be fitted by several sets of J's. One of the criteria of such a procedure is the prediction of the proper spin S value of the ground state, together with the location of the excited states, in particular the $S=9$ state. The χ_{dc} fit yielded at least two sets of J's, but the set providing the better fit yielded the position of the $S=9$ state to be less than 0.5 cm^{-1} above the ground state.[12] The other set predicted the $S=9$ state at greater than 25 cm^{-1} (36 K) above the ground state. From the point of view of understanding the magnetic structure of Fe_8Br_8, it is thus important to experimentally determine the location of the excited states, in particular the $S=9$ manifold. A peak around 30 cm^{-1} has been reported in the far-infrared spectrum,[25] but it was not established whether it was a normal molecular vibration involving metal ions or a transition to the $S=9$ level from the $S=10$ ground state. Moreover, this peak was not observed for the closely similar compound $Fe_8Br_4(ClO_4)_4$, whose spin Hamiltonian [Eq. (1)] parameters are known to be close to those of Fe_8Br_8.[25,26]

The magnetic properties of the ground state of Fe_8Br_8 have been well described by the following spin Hamiltonian, with $S=10$ (Refs. 6, 15–21, and 25–27):

$$\hat{H}=\mu_B\vec{B}\cdot\vec{g}\cdot\vec{S}+DS_z^2+E(S_x^2-S_y^2)+B_4^0O_4^0+B_4^2O_4^2+B_4^4O_4^4, \quad (1)$$

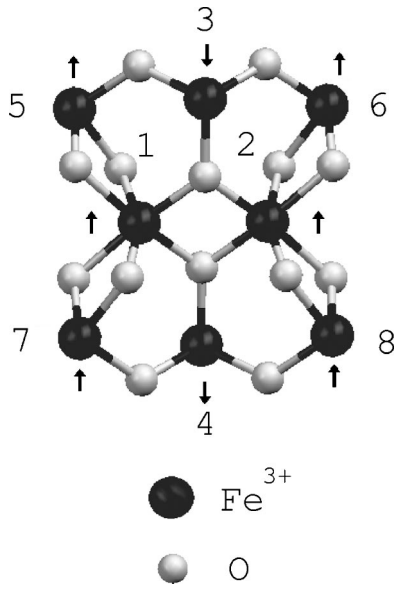

FIG. 1. Schematic representation of Fe_8Br_8 (Ref. 12). The arrows represent spin orientations of the Fe^{3+} ions in the $S=10$ ground state. The organic ligands and the eight Br^- anions have been omitted for clarity. Each Fe^{3+} has $S=5/2$; thus the ground state spin can be seen as $S=6\times5/2-2\times5/2=10$.

where the first term is the Zeeman interaction, D represents the usual zero-field uniaxial anisotropy parameter, and E the second-order rhombic anisotropy. The fourth-order terms are given by $O_4^0 = 35\,S_z^4 - [30\,S(S+1) - 25]S_z^2 - 6S(S+1) + 3\,S^2(S+1)^2$, $O_4^2 = 1/4[7S_z^2 - S(S+1) - 5](S_+^2 + S_-^2) + (S_+^2 + S_-^2)[7S_z^2 - S(S+1) - 5]$, and $O_4^4 = 1/2(S_+^4 + S_-^4)$.

Here, we report on an EPR detection of the $S=9$ state of Fe_8Br_8 and preliminary evaluation of its spin Hamiltonian parameters as defined in Eq. (1). We observe a series of peaks, called β transitions, which we assign to an $S=9$ excited state of Fe_8Br_8. From the temperature variation of the line intensities, we establish that the $S=9$ manifold lies at 24 ± 2 K above the $S=10$ ground state, in contrast to the suggestion of >36 K from susceptibility analysis.[12]

Section II below describes the single-crystal preparation and the EPR instrumentation. The results obtained and their analysis are presented in Sec. III, with the discussion presented in Sec. IV and the conclusions summarized in Sec. V.

II. EXPERIMENT

$[(C_6H_{15}N_3)_6\,Fe_8(\mu_3\text{-}O)_2(\mu_2\text{-}OH)_{12}]\,Br_7(H_2O)\,Br\cdot 8H_2O(Fe_8Br_8)$ was synthesized following the procedure of Weighardt *et al.*[10] Relatively large (2 mm$\times$2 mm $\times$0.5 mm), optical quality single crystals were prepared by slow evaporation. The crystals were aligned with the Zeeman field applied along the easy axis of magnetization by sight, to within a few degrees.[16] The final orientation was confirmed by EPR splittings, being the extremum for the canonical orientations. The EPR measurements were made using a variable-frequency (44–200 GHz), cavity-based, high-sensitivity spectrometer described earlier.[15,16,28] The main component of the spectrometer is a millimeter-wave vector network analyzer (MVNA), a phase-sensitive, fully sweepable, superheterodyne source-detection system. A variable-flow cryostat situated within the bore of a 17 T superconducting solenoid allows for temperatures down to 1.5 K, with an accuracy of ±0.01 K. The high sensitivity of the MVNA technique (10^9 spins $G^{-1}\,s^{-1}$) allows for observation of the low-level transitions of the Fe_8Br_8 ground and excited states in a single crystal and for angular variation studies, as described earlier.[6,15,21]

III. RESULTS

Figure 2 (bottom panel) shows a typical EPR spectrum of Fe_8Br_8 at 131 GHz with the Zeeman field applied along the easy axis of an Fe_8Br_8 single crystal at 35 K. The spectrum consists of a series of strong peaks α_{-10}, α_{-9}, α_{-8}, etc.; the subscripts represent the spin projection quantum number M_s, corresponding to the level from which the EPR absorption transition originates, in the $S=10$ ground state following the convention introduced earlier.[16,17] The α transitions have been very well analyzed earlier[16,17,21] and have been shown to arise from the magnetic dipole ($\Delta M_s = \pm 1$) transitions within the 21 M_s levels of the $S=10$ multiplet. The specific peak assignment is indicated in the top panel for the α transitions. In addition to the α resonances, there are additional

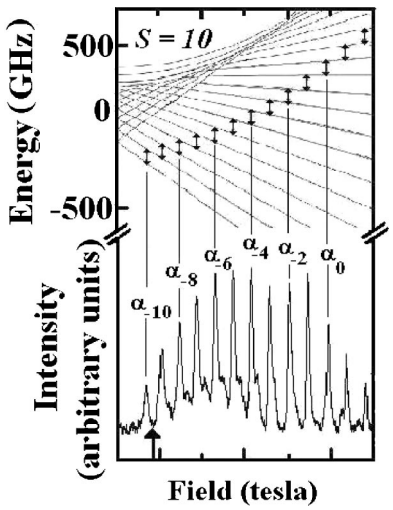

FIG. 2. EPR spectrum of Fe_8Br_8 at 131 GHz and 35 K with the Zeeman field applied along the easy axis (bottom panel), along with the energy level diagram corresponding to the $S=10$ spin system (top panel). The $S=10$ energy level diagram has been constructed through the spin Hamiltonian parameters of Caciuffo *et al.* (Ref. 13). The single-headed arrow at 0.8 T designates the expected position where a β_{10} would appear if the β transitions originated from an $S=10$ state.

peaks present in Fig. 2 that are labeled as the β transitions and are the focus of the current investigation.

Our analysis procedure consisted of three steps: (a) to ascertain that the β transitions are from an excited state, (b) to determine the spin multiplicity of this excited state, and (c) to deduce the spin Hamiltonian parameters for the β spin system and its energy position relative to the ground state ($S=10$).

Direct evidence that the β transitions originate from a thermally populated excited state is provided by the temperature dependence of their intensities. Figure 3 shows spectra at 5, 15, and 35 K, respectively, giving clear experimental evidence that the β transitions arise from a thermally populated excited state, because their intensities rapidly decrease as the temperature is lowered.

In order to quantitatively measure the intensities of the β peaks as a function of temperature, the spectra of the ground and excited states needed to be separated. The separation was accomplished by using a Gaussian fit for each individual peak. The validity of Gaussian fits, especially for the low-field transitions, has been previously established.[21] The criterion for the goodness of the fit was that the sum of the α and β transitions mirrors the experimental data quite well by visual inspection and also by minimizing the remaining intensity obtained by subtracting the Gaussian fits from the experimental spectra. This remaining intensity was within the experimental noise in our separation procedure. Each Gaussian fit was then summed to yield a separated $S=10$ spectrum. The spectra were then separated by subtracting the Gaussian fits of the α peaks from the experimental spectra. The remaining β peaks were then fit with Gaussian functions and summed, yielding a separated $S=9$ spectrum. We verified that these separated spectra agreed well with the experi-

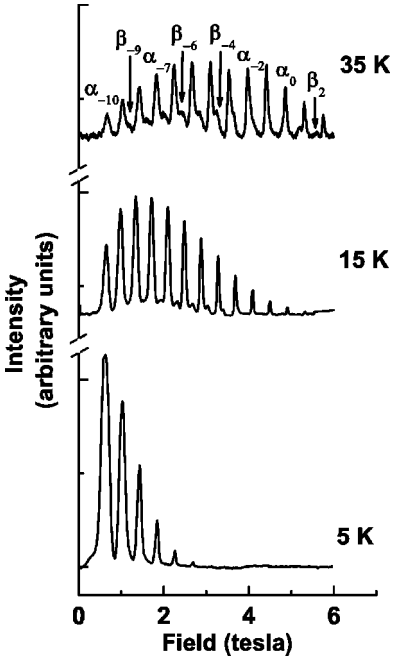

FIG. 3. Temperature dependence of EPR spectra of Fe_8Br_8, for $B\|z$ at 131 GHz and 5, 15, and 35 K.

mental data by taking the sum of the α and β spectra and comparing it with experiment, as shown in Fig. 4(a).

Figure 4 also shows the relative decrease in the intensity of the separated excited-state (β) spectra in relation to the $S=10$ spectra as the temperature is decreased. The spectral envelope present in the $S=10$ spectra at 5, 15, and 35 K is

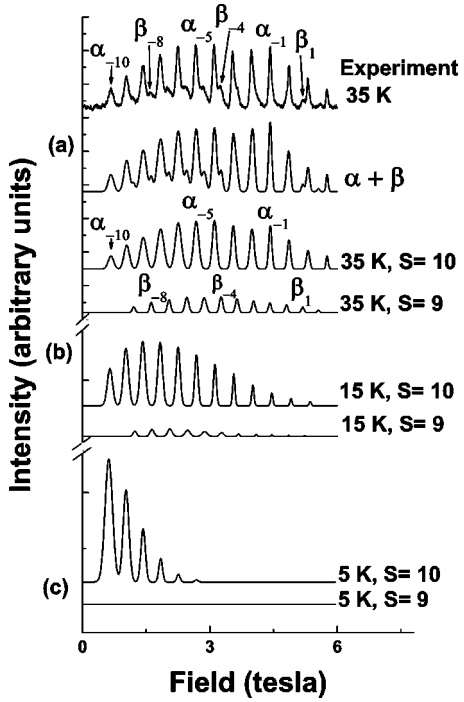

FIG. 4. (a) Experimental, resummed α and β, separated $S=9$, and separated $S=10$ spectra at 35 K and 131 GHz for $B\|z$. (b) Separated spectra at 15 K, (c) and at 5 K.

generally evident in the corresponding excited-state spectra, though the relative intensities are modified slightly due to differing matrix elements in the transition probabilities, $P_{nm}\propto|\langle\psi_n|S_+|\psi_m\rangle|^2$, of the two spin systems, given by Eq. (2):

$$P\propto[S\times(S+1)-M_s\times(M_s+1)]. \tag{2}$$

In order to analyze the intensity of the β peaks we normalized their intensities. The normalization process involved dividing the intensity of a β peak, with a given M_s value, by the corresponding α peak with the same M_s value. This enabled us to ignore instrumental effects and spectral envelope changes with temperature. At 5 K, the β peaks are barely discernable from the noise level of the spectrum. At 10 K, however, they increase in intensity enough to emerge from the α transitions. The decreasing intensity of the β peaks, upon lowering temperature, unambiguously designate the β peaks as being due to a thermally populated excited state.

Once it was concluded that the β peaks originated from an excited state, the spin multiplicity of the excited state needed to be determined. The presence of an excited state (with perhaps $S=9$) close to the ground state of Fe_8Br_8 has been previously inferred from magnetic susceptibility[12] and mentioned in subsequent muon spin relaxation (μSR),[24] EPR,[26] and neutron diffraction studies,[29] without any evidence for its location or multiplicity. Herein, the spin multiplicity of the excited state has been determined by two independent methods: first, by the location of the leading peak (β_{-9}) in the set of peaks assigned to the $S=9$ state. Figure 2 shows an experimental spectrum taken at 131 GHz and 35 K. As is evident in all spectra taken, there is no β peak between the α_{-10} and α_{-9} peaks. Furthermore, the α_{-10} transition is symmetric and shows a clear Gaussian shape, as would be expected at this temperature for a well separated, individual peak.[21] This lack of a β_{-10} transition, barring spin Hamiltonian parameters being very different from those for the ground state, is strong evidence that the excited state is $S=9$. The location of the first β peak is consistent with slightly modified spin Hamiltonian parameters and a spin multiplicity of $S=9$ for the excited state, as anticipated theoretically.[12]

Additional, more quantitative support—that the spin S of this excited state is indeed $S=9$—was provided by computer simulations which were run using SIM.[30] The procedure was first checked for the $S=10$ state for which the parameters are known.[13,17,21,25] The simulations for the $S=10$ state were performed with the spin Hamiltonian parameters previously determined by Caciuffo *et al.*[13] using neutron scattering. A typical comparison is shown in Fig. 5. The simulated spectra for the $S=10$ ground state were in close agreement with our experimental results, thereby validating the simulation procedure.

The β transitions were then accurately simulated for the three frequencies utilized (110, 131, and 155 GHz), using the spin Hamiltonian parameters obtained in the present study. A field-frequency plot is shown in Fig. 6. Quite good agreement can be seen between the simulated curves (solid lines) and the observed peak positions. A more explicit and quan-

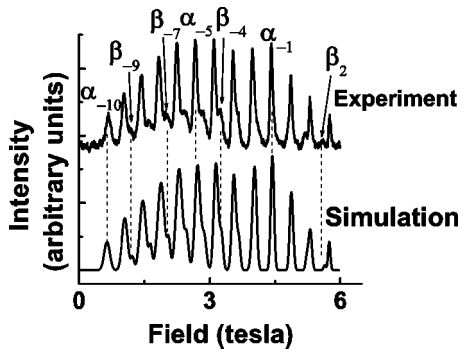

FIG. 5. Experimental and simulated EPR spectra of Fe_8Br_8, for $B\|z$ at 35 K and 131 GHz.

titative comparison is shown in Table I, using the measured data for 131 GHz. The D parameter decreases in magnitude by 8%, to -0.27 K, while the E term increases by 7%, to ± 0.05 K (± 0.015 K). Surprisingly, the B_4^0 term is similar in magnitude, -1.3×10^{-6} K, but opposite in sign to the $S=10$ parameter (1.01×10^{-6} K). Due to the fact that the experimental spectra were taken along the easy axis of magnetization, the B_4^2 and B_4^4 terms were not included in the simulations. A simulated spectrum at 35 K, with the spin Hamiltonian parameters determined for both the $S=10$ and $S=9$ states, is shown in Fig. 5. Linewidths were not an optimized parameter in the simulations, though the relative intensities matched the experimental data well. Therefore, the simulated spectrum presented in this figure is the sum of the $S=10$ and $S=9$ separated spectra using peak positions generated by SIM.[30] The agreement between the experimental and simulated spectra, as shown in Fig. 5, can be seen to be quite satisfactory, thereby supporting the parameter assignment. We are thus able to assign the full experimental spectrum to transitions in the $S=10$ multiplet (α's) and the $S=9$ multiplet (β's).

Once the spin Hamiltonian parameters had been determined, the relative intensities of the α and β transitions were used, at temperatures from 5 to 35 K, to determine the location of the $S=9$ state above the ground state. The intensity

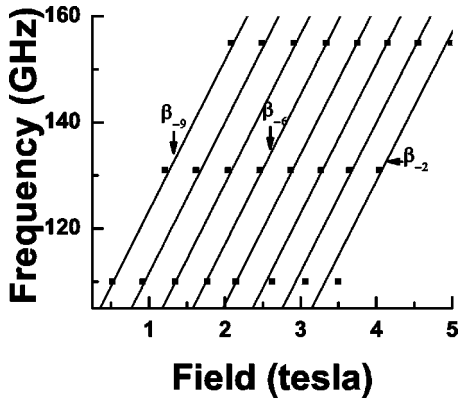

FIG. 6. Frequency dependence of the first eight β transitions in Fe_8Br_8 with $B\|z$. The solid lines portray the frequency dependence given by the spin Hamiltonian parameters determined in this work, whereas the solid squares are the observed field positions.

TABLE I. Experimental and simulated peak positions at 131 GHz for the $S=9$ state, for $B\|z$, using $D=-0.27$ K, $E=\pm0.05$ (±0.015) K, $B_4^0=-1.3\times10^{-6}$ K, $B_4^2=0$ K, and $B_4^4=0$ K.

Transition $M_s\rightarrow M_{s+1}$	Experiment (tesla)	Simulation (tesla)
$-9\rightarrow-8$, β_{-9}	1.2082	1.2282
$-8\rightarrow-7$, β_{-8}	1.6208	1.6400
$-7\rightarrow-6$, β_{-7}	2.0409	2.0608
$-6\rightarrow-5$, β_{-6}	2.4610	2.4691
$-5\rightarrow-4$, β_{-5}	2.8679	2.8727
$-4\rightarrow-3$, β_{-4}	3.2659	3.2760
$-3\rightarrow-2$, β_{-3}	3.6394	3.6721
$-2\rightarrow-1$, β_{-2}	4.0312	4.0585
$-1\rightarrow0$, β_{-1}	4.4126	4.4571

of a specific peak between given M_s and M_{s+1} states, is proportional to the population difference between the M_s and M_{s+1} states and the transition probability P as given in Eq. (3):

$$I\propto P(N_{M_s}-N_{M_{s+1}})/Z. \tag{3}$$

Therefore, assuming very similar partition functions and D values for the two states, the intensity ratio between two transitions of the same M_s states in the $S=9$ and $S=10$ manifolds, respectively, is given by

$$I_9/I_{10}=(P_9/P_{10})\exp(-\Delta E_{10-9}/kT), \tag{4}$$

where k is the Boltzmann constant and ΔE_{10-9} is the energy difference between given M_s states in the $S=10$ and $S=9$ manifolds. The areas of the Gaussian fits, for a given M_s to M_{s+1} transition, were factored by their transition probabilities, in both the $S=9$ and $S=10$ manifolds, in order to determine their ratios. Due to the fact that each β transition is normalized to its corresponding α transition, the ratio of intensities should be constant, regardless of the specific M_s pair, for any given temperature.

A Boltzmann analysis of the intensity ratios is shown in Fig. 7(b). The ratios of intensities of the β to α transitions were compared at 5, 15, 20, 25, 30, and 35 K and plotted versus inverse temperature (T^{-1}). The slope yields the energy difference (18 K) between a given $M_s(9)$ state and the corresponding $M_s(10)$ state. Therefore, the energy difference between the $M_s=10$ and $M_s=9$ ($S=10$) in zero field (5.46 K) must be added to the energy obtained from the Boltzmann analysis, yielding an energy difference Δ of 24 ± 2 K (17 ± 1.5 cm^{-1}). Figure 8 shows a schematic of the energy levels in zero field for the $S=10$ and $S=9$ manifolds based on the present study. Clearly, the higher M_s levels of the $S=9$ state overlap with the lower M_s levels of the $S=10$ state, indicating at least a partial breakdown of the single-spin model.

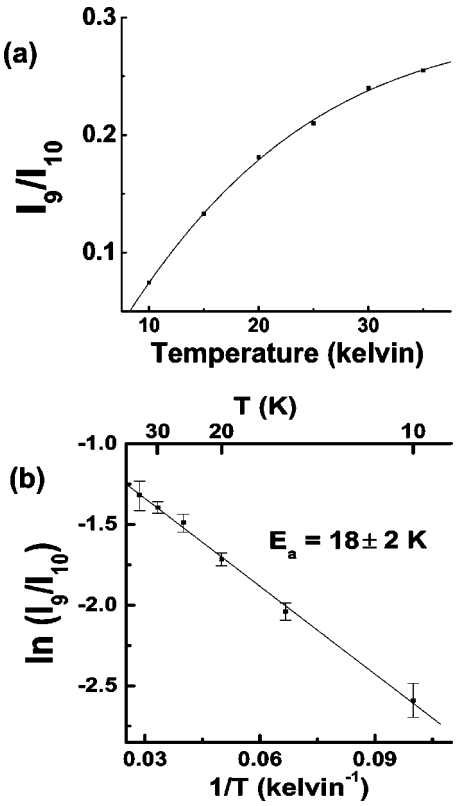

FIG. 7. (a) Temperature dependence of the intensity of the -8 to -7 transition in the $S=9$ state, I_9, normalized to the -8 to -7 transition in the $S=10$ state, I_{10}. The curve joining the experimental points is a guide to the eye. (b) Boltzmann analysis of the normalized intensities of the $S=9$ spin state. The slope yields the excitation energy as 18 ± 2 K between level with the same M_s values in the $S=10$ and $S=9$ manifolds. Addition of the zero-field splitting between the $M_s=-10$ and $M_s=-9$ levels (5.5 K) leads to the location of the $S=9$ state at 24 ± 2 K above the ground state.

IV. DISCUSSION

Our determination that the $S=9$ manifold in Fe_8Br_8 is located 24 ± 2 K above the $S=10$ ground state is in contrast to with earlier suggestions based on magnetic susceptibility (>36 K).[12] The four central Fe^{3+} ions in the Fe_8Br_8 core [Fe_1^{3+}, Fe_2^{3+}, Fe_3^{3+}, and Fe_4^{3+} (as shown in Fig. 1)] can be described as that of a butterfly configuration. All magnetic coupling interactions J between Fe^{3+} ions in Fe_8Br_8 have been determined to be antiferromagnetic.[12] Therefore, the magnitude of these coupling constants dictates both the location and spin topology of the $S=9$ excited state.

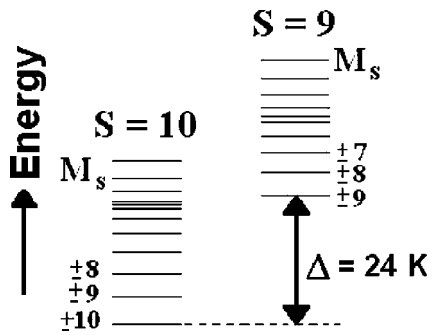

FIG. 8. Schematic for the energy levels of both the $S=10$ and the $S=9$ states in zero magnetic field. $S=9$ is located at an energy $\Delta=24\pm2$ K as marked.

As mentioned in the Introduction, a detailed analysis of the dc magnetic susceptibility data led Delfs *et al.*[12] to two reasonable sets of exchange parameters: (a) $J_{1-2}=20$ cm^{-1}, $J_{1-3}=120$ cm^{-1}, $J_{1-5}=15$ cm^{-1}, and $J_{3-5}=35$ cm^{-1} and (b) $J_{1-2}=102$ cm^{-1}, $J_{1-3}=120$ cm^{-1}, $J_{1-5}=15$ cm^{-1}, and $J_{3-5}=35$ cm^{-1}. While set (b) provided a much better fit to the experimental data, it predicted the position of the first excited state, $S=9$, at less than 0.5 cm^{-1} above the $S=10$ ground state. We do note, however, that Delfs *et al.* did not include any zero-field splitting terms in their susceptibility analysis. Nevertheless, this same basic configuration of exchange constants has been recently supported by detailed symmetry-based calculations by Raghu *et al.*[31] Though the magnitudes of the coupling constants calculated by these authors[31] are different from those of Delfs *et al.*,[12] the dominance of the J_{1-3} interaction over other magnetic couplings remains consistent. The present study supports the essential correctness of set (a), cautioning about the use of χ-fitting alone to determine the J's.

The coupling set (a) of Delfs *et al.*[12] and the best set of Raghu *et al.*[31] both show that J_{1-3} dominates the exchange interactions. The perturbation leading to the $S=9$ excited state must result from the smallest difference in J's acting on the same ion or symmetrically equivalent set of Fe^{3+} ions. Thus it seems reasonable to deduce that this perturbation does not involve J_{1-3}, hence the butterfly core (Fe_1, Fe_2, Fe_3, Fe_4), but rather the Fe's on the corners of the cluster (Fe_5, Fe_6, Fe_7, Fe_8) via some linear combination of their wave functions.

The spin Hamiltonian parameters determined for the $S=9$ state provide some insight into the origin of the anisotropy of the cluster. The $S=9$ parameters are slightly different from those of the $S=10$ ground state. The 7% larger E value for $S=9$ is in accordance with increased transverse distortion in the Fe_8 structure. The decrease in D with decreasing magnetic moment indicates that the anisotropy present in the Fe_8Br_8 core has some dipolar contribution rather than arising purely from a spin-orbit interaction. Similarly, the change in sign of the B_4^0 term indicates that B_4^0 originates from many-body interactions between Fe^{3+} ions, and not from a collective sum of individual B_4^0 terms. This argument is in line with the fact that a B_4 term needs an effective interaction involving at least four spins. Alternatively, this significant change in B_4^0 may be a result of the breakdown of the single-spin model, as has been proposed by Katsnelson *et al.* in connection with Mn_{12}-acetate.[32] Additional, detailed angular variation studies are underway for precise measurement and understanding of these questions.

The anisotropy barrier, estimated from D and E values for the $S=9$ manifold, is 22 K, as compared to that for the $S=10$ ground state (29 K).

V. CONCLUSIONS

Using variable-frequency, high-field, EPR measurements on single crystals of Fe_8Br_8, we have detected a set of tran-

sitions, labeled as β_i, which have been conclusively assigned to the $S=9$ spin multiplet, located at an energy $\Delta = 24 \pm 2$ K (17 ± 1.5 cm^{-1}) above the ground ($S=10$) state. The spin Hamiltonian parameters have been determined to a good accuracy and differ from those of the $S=10$ state: D is smaller by 8%, while E is larger by 7%. These parameters yield the anisotropy barrier ($\sim DS_z^2 \sim 22$ K), about 25% smaller than for $S=10$. B_4^0 for $S=9$ also shows a dramatic change; the sign is opposite to that for the $S=10$ state. Although electronic structure calculations have been reported for Fe_8Br_8,[31,33,34] there has been little definitive data on excited states. The results of the present study should serve as a sensitive basis for more refined theoretical modeling of the bonding and magnetic properties of these materials.

ACKNOWLEDGMENT

We would like to thank the National Science Foundation (NIRT Grant No. DMR 0103290) for financial support. S.H. would also like to thank the National Science Foundation DMR (Grant Nos. 0196430 and 0239481) and Research Corporation.

[1] R. Sessoli, D. Gatteschi, A. Caneschi, and M.A. Novak, Nature (London) **365**, 141 (1993).
[2] M.A. Novak, R. Sessoli, A. Caneschi, and D. Gatteschi, J. Magn. Magn. Mater. **146**, 211 (1995).
[3] J.R. Friedman, M.P. Sarachik, J. Tejada, and R. Ziolo, Phys. Rev. Lett. **76**, 3830 (1996).
[4] C. Sangregorio, T. Ohm, C. Paulsen, R. Sessoli, and D. Gatteschi, Phys. Rev. Lett. **78**, 4645 (1997).
[5] J.A.A.J. Perenboom, J.S. Brooks, S. Hill, T. Hathaway, and N.S. Dalal, Phys. Rev. B **58**, 330 (1998).
[6] S. Hill, R.S. Edwards, S.I. Jones, N.S. Dalal, and J.M. North, Phys. Rev. Lett. **90**, 217204 (2003).
[7] M.R. Cheesman, V.S. Oganesyan, R. Sessoli, D. Gatteschi, and A.J. Thompson, Chem. Commun. (Cambridge) **17**, 1677 (1997).
[8] E.M. Chudnovsky and J. Tejada, *Macroscopic Quantum Tunneling of the Magnetic Moment* (Cambridge University Press, Cambridge, England, 1998).
[9] M.N. Leuenberger and D. Loss, Nature (London) **410**, 789 (2001).
[10] K. Weighardt, K. Pohl, I. Jibril, and G. Huttner, Angew. Chem., Int. Ed. Engl. **23**, 77 (1984).
[11] A.L. Barra, P. Debrunner, D. Gatteschi, C.E. Schulz, and R. Sessoli, Europhys. Lett. **35**, 133 (1996).
[12] C. Delfs, D. Gatteschi, L. Pardi, R. Sessoli, K. Weighardt, and D. Hanke, Inorg. Chem. **32**, 3099 (1993).
[13] R. Caciuffo, G. Amoretti, A. Murani, R. Sessoli, A. Caneschi, and D. Gatteschi, Phys. Rev. Lett. **81**, 4744 (1998).
[14] S. Carretta, E. Liviotti, G. Amoretti, R. Caciuffo, A. Caneschi, and D. Gatteschi, Phys. Rev. B **65**, 052411 (2002).
[15] S. Hill, J.A.A.J. Perenboom, N.S. Dalal, T. Hathaway, T. Stalcup, and J.S. Brooks, Phys. Rev. Lett. **80**, 2453 (1998).
[16] S. Maccagnano, R. Achey, E. Negusse, A. Lussier, M.M. Mola, S. Hill, and N.S. Dalal, Polyhedron **20**, 1441 (2001).
[17] A.L. Barra, D. Gatteschi, and R. Sessoli, Chem.-Eur. J. **6**, 1608 (2000).
[18] E. del Barco, J.M. Hernandez, J. Tejada, N. Biskup, R. Achey, I. Rutel, N.S. Dalal, and J.S. Brooks, Phys. Rev. B **62**, 3018 (2000).
[19] R. Blinc, P. Cevc, D. Arcon, N.S. Dalal, and R.M. Achey, Phys. Rev. B **63**, 212401 (2001).
[20] K. Park, M.A. Novotny, N.S. Dalal, S. Hill, and P.A. Rikvold, Phys. Rev. B **65**, 014426 (2002).
[21] S. Hill, S. Maccagnano, K. Park, R.M. Achey, J.M. North, and N.S. Dalal, Phys. Rev. B **65**, 224410 (2002).
[22] Y. Furukawa, K. Kumagai, A. Lascialfari, S. Aldrovandi, F. Borsa, R. Sessoli, and D. Gatteschi, Phys. Rev. B **64**, 094439 (2001).
[23] W. Wernsdorfer and R. Sessoli, Science **284**, 133 (1999).
[24] A. Lascialfari, P. Carretta, D. Gatteschi, C. Sangregorio, J.S. Lord, and C.A. Scott, Physica B **289-290**, 110 (2000).
[25] A. Mukhin, B. Gorshunov, M. Dressel, C. Sangregorio, and D. Gatteschi, Phys. Rev. B **63**, 214411 (2001).
[26] A.L. Barra, F. Bencini, A. Caneschi, D. Gatteschi, C. Paulsen, C. Sangregorio, R. Sessoli, and L. Sorace, Chem. Phys. Chem. **2**, 523 (2001).
[27] A. Abragam and B. Bleaney, *Electron Paramagnetic Resonance of Transition Ions* (Dover, New York, 1986).
[28] (a) S. Hill, N.S. Dalal, and J.S. Brooks, Appl. Magn. Reson. **16**, 237 (1999); (b) M. Mola, S. Hill, P. Goy, and M. Gross, Rev. Sci. Instrum. **71**, 186 (2000).
[29] Y. Pontillon, A. Caneschi, D. Gatteschi, R. Sessoli, E. Ressouche, J. Schweizer, and E. Lelievre-Berna, J. Am. Chem. Soc. **121**, 5342 (1999).
[30] Simulation software by Dr. H. Weihe; for more information see http://sophus.kiku.dk/software/epr/epr.html
[31] C. Raghu, I. Rudra, D. Sen, and S. Ramasesha, Phys. Rev. B **64**, 064419 (2001).
[32] M.I. Katsnelson, V.V. Dobrovitski, and B.N. Harmon, Phys. Rev. B **59**, 6919 (1999).
[33] J. Kortus, M.R. Pederson, C.S. Hellberg, and S.N. Khanna, Eur. Phys. J. D **16**, 177 (2001).
[34] M.R. Pederson, J. Kortus, and S.N. Khanna, J. Appl. Phys. **91**, 7149 (2002).